Cover Sheet for EarthAriv

Title:

Production and Preservation of Lipid Biosignatures in SO4-Rich Hypersaline Lakes of the Cariboo Plateau

Authors:

Floyd Nichols - Department of Earth and Planetary Sciences, Northwestern University, Evanston IL, USA

Alexandra Pontefract - Space Exploration Sector, Johns Hopkins University Applied Physics Laboratory, Laurel MD, USA

Hannah Dion-Kirschner - Division of Geological and Planetary Sciences, California Institute of Technology, Pasadena CA, USA

Andrew L. Masterson - Department of Earth and Planetary Sciences, Northwestern University, Evanston IL, USA; United States Geological Survey, Reston Virginia, USA

Magdalena R. Osburn - Department of Earth and Planetary Sciences, Northwestern University, Evanston IL, USA

Author Email Addresses:

Floyd Nichols (floydnichols2025@u.northwestern.edu)

Alexandra Pontefract (alexandra.pontefract@jhuapl.edu)

Hannah Dion-Kirschner (hannahdk@caltech.edu)

Andrew L. Masterson (andrew.masterson@northwestern.edu)

Magdalena R. Osburn (maggie@northwestern.edu)

Peer Review Statement:

This is a non-peer-reviewed preprint submitted to EarthArXiv. the work has been submitted to the Journal of Geophysical Research Biogeosciences for review.

Production and Preservation of Lipid Biosignatures in SO_4-Rich Hypersaline Lakes of the Cariboo Plateau

Floyd Nichols[1+], Alexandra Pontefract[2], Hannah Dion-Kirschner[3], Andrew L. Masterson[1,4], Magdalena R. Osburn[1+]

[1] Department of Earth and Planetary Sciences, Northwestern University, Evanston IL, USA

[2] Space Exploration Sector, Johns Hopkins University Applied Physics Laboratory, Laurel MD, USA

[3] Division of Geological and Planetary Sciences, California Institute of Technology, Pasadena CA, USA

[4] United States Geological Survey, Reston Virginia, USA

+ corresponding authors [floydnichols2025@u.northwestern.edu; maggie@northwestern.edu]

Key Points

- Sulfate-dominated hypersaline lakes produce and preserve organic matter better than a Na-CO_3 dominated site of comparable salinity.
- Sediments contain more diverse and abundant lipids than water column samples suggesting preferential degradation and preservation in the sediments.
- Microbial biosignatures produced *in situ* predominate in all lakes rather than those produced by surrounding vegetation.

Abstract

Modern and ancient hypersaline lakes and oceans have been identified across the solar system, but the habitability and potential of these environments to preserve organic matter remain unknown. Here, we evaluate organic matter production and preservation potential in hypersaline lakes whose chemistries resemble deposits on Mars. We focus our analysis on lipid biomarkers including fatty acids, alkanes, and ether-bound lipids in modern brines, salt deposits, and surface sediments. We also report total organic carbon (TOC), carbon/nitrogen (C/N) ratios, and bulk OC ($\delta^{13}C$ and $\delta^{15}N$) isotopes to contextualize the lipid data. In all lakes, the predominant biosignatures include short chain fatty acids (C<23) suggesting microbial origin. Sediments also incorporate a diversity of microbially and terrestrially derived lipids. Ether-bound lipids derived from archaea and bacteria constitute a minor but measurable fraction of the lipids in brines. This result contrasts with typical results from NaCl brines which contain significant archaeal biomass. TOC concentrations in sediments are universally high, ranging from 0.7% to 12% with sulfate-rich sediments having the highest concentrations. The isotopic composition of TOC corroborates the biomarker results, showing $\delta^{13}C$ values and C/N values indicative of aquatic microbial origin. This richness of organic material and *in situ* microbial biosignatures differ from previously studied Cl-dominated Mars-analog sites which have shown limited organic matter production and preservation and acidic SO_4-rich hypersaline environments which were dominated by terrestrial inputs. Overall, our results suggest that Mg-SO_4-rich hypersaline environments harbor a rich microbial biomarker landscape and are ideal locations for preserving these signatures, potentially over geological timescales.

Plain Language Summary

The minerals found on Mars suggest that it had abundant hypersaline waters early in its history. However, liquid water no longer persists on its surface. As such, we must use environments on Earth that are similar to Mars and other astrobiological targets to better understand the potential for life elsewhere. Here, we examine fatty molecules from hypersaline lakes on Earth that resemble water compositions thought to have been present on Mars. We also use bulk carbon isotopic data and total organic carbon to help inform the results from our biomarker analysis. Overall, data from these sites shows a well-preserved microbial organic matter

signature. In comparison to other Martian-analog environments on Earth, this study shows that sulfate-dominated lakes produce and preserve *in situ* biological signatures in abundance.

1. Introduction

Detection of past or present life beyond Earth is a primary driver of mission-based planetary science. As life detection efforts push forward, an emphasis on habitability is imperative (Kite *et al*., 2018). Previous work on extreme environments on Earth have identified environmental parameters that may limit habitability such as evidence for syndepositional desiccation, perchlorate salts, acidic fluids, and/or hypersaline fluids (Carrizo *et al*., 2019, Wilhelm *et al*., 2017, Hallsworth *et al*., 2007). Specifically for hypersaline environments, habitability is affected by ionic strength (concentration of ions in solution), water activity (a_w, thermodynamic availability of water), and lyotropic properties (ion specific behavior in aqueous solutions) of solutes (Pontefract et al. 2017; Fox-Powell 2016). These factors ultimately govern the production and stability of organic matter (OM) and therefore preservation potential of biosignatures in resultant deposits. Most hypersaline lakes on Earth are dominated by NaCl where the Cl^- anion is chaotropic or membrane destabilizing (Pontefract *et al*., 2017; Hallsworth *et al*., 2007). Additionally, many Mars-analog hypersaline lakes that are Cl-dominated are paired with the Ca^{2+} or Mg^{2+} cation (e.g., Don Juan Pond in Antarctica, the Discovery Basin in the Mediterranean, and the South Bay Salt Work Bitterns in Southern California) which can be highly chaotropic solutes depending on the organic molecule in question. These sites contain some of the lowest biomass levels found on Earth, with correspondingly low microbial diversity and organic content (Klempay *et al*., 2021; Dickson *et al*., 2013; Hallsworth *et al*., 2007). While these studies are informative, many of these sites resemble modern-day Martian environments rather than those that encompass conditions present deeper in its history (Ehlmann *et al*., 2008). The viability of life and preservation of biosignatures by other ions that are kosmotropic or membrane stabilizing such as SO_4 remain poorly constrained (Fox-Powell & Cockell, 2018; Pontefract, 2017; Tosca *et al*., 2008; Hallsworth *et al*., 2007).

Extremely SO_4-rich aqueous environments are rare on Earth, yet key astrobiological targets on Mars host ancient evaporite deposits thought to be comprised of SO_4 and Mg-rich salts (Fox-Powell & Cockell, 2018; Pontefract *et al*., 2017; Barbieri *et al*, 2014; Tosca *et al*., 2008; Aubrey *et al*., 2006). Environments with these fluid chemistries are known on Earth from South-Central,

British Columbia and Western Australia which each host a variety of such systems (Johnson *et al*., 2020; Pontefract *et al*., 2017). Previous work on these Mars-analog environments has shown a range of OM production, preservation, or microbial activity. Work done using metagenomic analysis in Spotted Lake (South-Central British, Columbia), a circumneutral Mg-SO_4 lake, showed the microbial community to be quite diverse and abundant (Pontefract *et al*., 2017). Lipid biomarkers are key tools to understand the astrobiological potential of these environments, due to their specificity to life and ability to be preserved on long geologic time scales (Johnson *et al*., 2017; Brocks & Pearson, 2005). Analysis of lipid biomarkers in acidic sulfate-rich lakes including Lake Gneiss and Lake Gilmore (Western Australia) showed very low biomass, diversity, and preservation (Johnson *et al*., 2020). Although these lakes are saturated with $MgSO_4$, the acidic conditions likely contributed to the very low concentrations of microbial lipids, especially short saturated and branched fatty acids. The dominant preserved lipid signatures here were long chain *n*-alkanes and fatty acids, reflecting selective preservation of terrestrial vegetation inputs.

There remains a knowledge gap surrounding the production and preservation of OM in circumneutral to alkaline SO_4-dominated hypersaline Mars analog environments, as few studies target these systems (Fox-Powell & Cockell, 2018; Pontefract *et al*., 2017) and even fewer have probed their OM preservation potential (Johnson *et al*., 2020; Benison *et al*, 2014). Results thus far are promising. For instance, Cheng *et al*. (2017) showed bacterial and Archaeal lipids are well preserved in terrestrial SO_4 salts and microorganisms such as diatoms and algae have been described from within fluid inclusions of gypsum ($CaSO_4 \cdot 2H_2O$; Benison *et al*, 2014). However, the controls on organic biosignature preservation and early diagenetic alteration under hypersaline conditions are unclear. Constraining the preservation potential of OM in terrestrial SO_4 and Mg-rich hypersaline lakes is necessary to inform the search for extraterrestrial life due to their kosmotropic potential. Here, we evaluate the production and preservation potential of OM in the kosmotropic Mars analog hypersaline lakes of the Cariboo Plateau, British Columbia using a lipid biomarker and isotope organic geochemistry approach.

2. Site Description

The lakes targeted here are situated on the Cariboo Plateau of South-Central Interior British Columbia, Canada between the Coast and Columbia-Rocky mountain ranges. Numerous lakes formed in this region ~10,000 years ago as glacial retreat produced closed basins with limited

drainage (Pontefract *et* al., 2017; Renaut & Long, 1989). Most of these lakes, including those studied here are principally groundwater-fed, with additional contributions from precipitation. (Renaut, 1990; Renaut & Long, 1989). This region is situated in the rain shadow of the Coast Mountains producing a semi-arid to sub-humid climate with an average annual precipitation of 300-400 mm yr^{-1} (Renaut & Long, 1989). The region also experiences extreme annual temperature ranges with average daily highs up to 35ºC in the summer, and temperatures as low as -40ºC in the winter (Renaut, 1993). These conditions produce ephemeral lakes that dry completely. Our three focus areas include the Basque Lakes (Basque Lake #1: 50º36'1.8" N, 121º21'32.4" W, Basque Lake #2: 50º35'36.6" N, 121º20'58.2" W, and Basque Lake #4: 50º35'20.304" N, 121º20'34.397" W), Clinton (Salt) Lake: 51º04'25.44" N, 121º35'11.244" W, and Last Chance Lake: 51º19'40.8" N, 121º38'9.6" W (Fig. 1). The chemical compositions of the brines in these systems are controlled by groundwater mediated bedrock dissolution: the Basque Lakes and Salt Lake are underlain by greenschist facies, and Paleozoic-Mesozoic metasediments of the Chilcotin Group (Salt Lake) respectively, and Venables Valley assemblage (Basque Lakes), including abundant localized pyrite deposits, whereas Na-CO_3-SO_4-Cl rich lake (Last Chance Lake) are underlain by basalts of the Chilcotin Group and surficial glacial sediments (Cui *et al*., 2017; Renaut & Long, 1989). As a result of this, high levels of Mg^{2+} and SO_4^{2-} are present in the groundwater, and are concentrated to saturation through evaporation during the summer months.

The lakes in this study are also unique in the world, featuring a distinctive "spotted" appearance with numerous separate but adjoining brine pools forming within each basin (Fig. 1; Pontefract *et al*., 2017; Renaut, 1990; Renaut & Long, 1989; Jenkins, 1918). The origin and structure of these spots is a matter of debate (Renaut, 1990) and is being investigated as part of our ongoing research (Fleugel et al., *in prep*). Brief comment on how the separated pools contribute to heterogeneity? Despite the aridity, heavily vegetated catchment areas surround many of these lakes featuring conifer forests and grassland assemblages, indicating that the salinity is not an impedance.

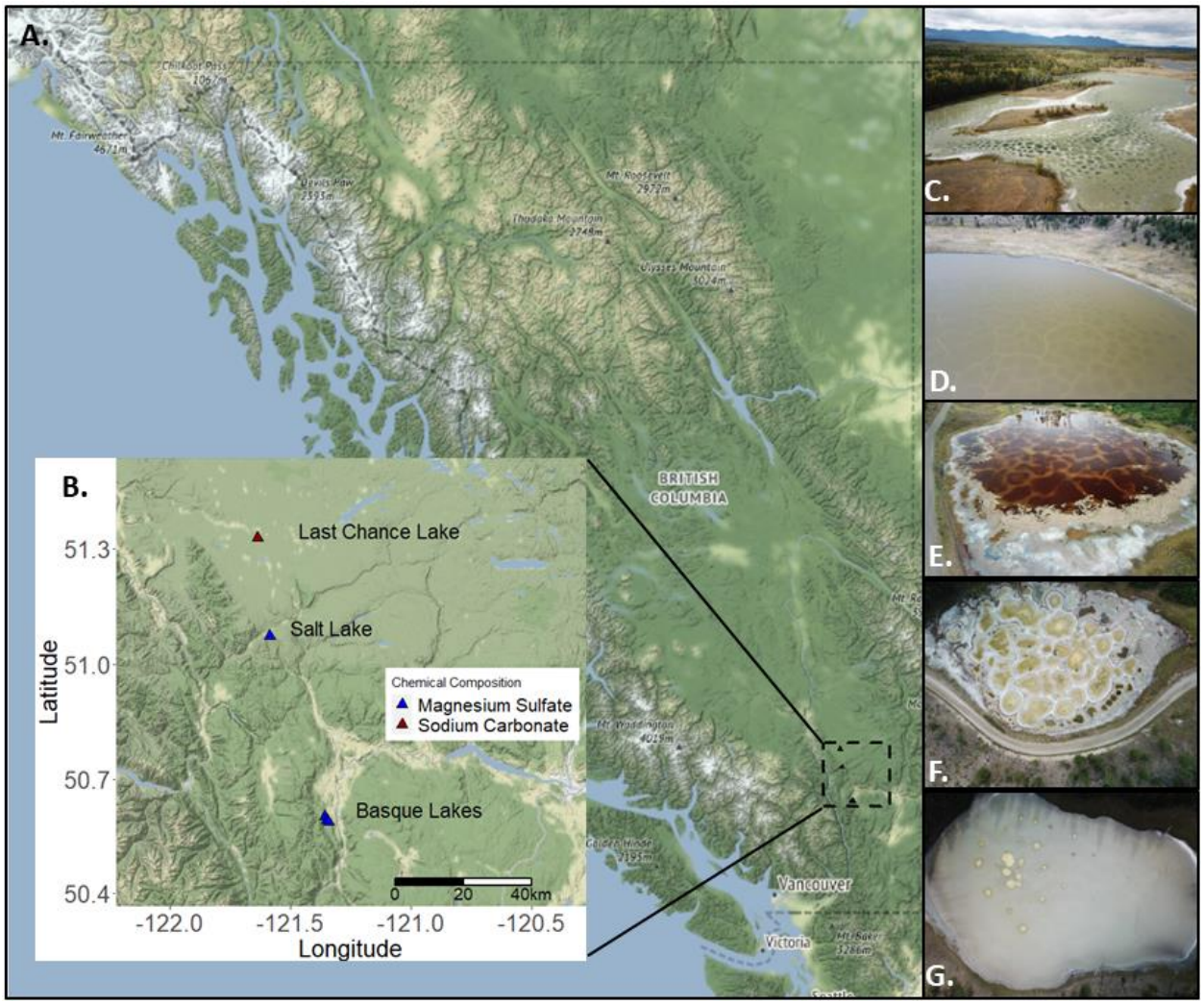

Figure 1. Map of study site. (A.) Province of British Columbia, Canada and (B.) inset of part of the Cariboo Plateau. Aerial photographs of the lakes studied: (C.) Last Chance Lake: 51º19'40.8" N, 121º38'9.6" W (D.) Salt Lake: 51º04'25.44" N, 121º35'11.244" W, (E.) Basque Lake #1: 50º36'1.8" N, 121º21'32.4" W (F.). Basque Lake #2: 50º35'36.6" N, 121º20'58.2" W (G.) Basque Lake #4: 50º35'20.304" N, 121º20'34.397" W. Photo credit: Mitchell Barklage. Map created using the package ggmaps in R.

3. Materials & Methods

3.1 Sampling

We sampled water, surface sediment, and salt from the Basque Lakes, Salt Lake, and Last Chance Lake in summer 2018, winter 2019, and summer 2019. Physicochemical measurements of the brines including pH, total dissolved solid (TDS), temperature, oxidation reduction potential (ORP), and conductivity were measured before sample collection using both a portable YSI probe and a Hanna Multiparameter Meter. Water activity was measured on-site using an AquaLab 4TE water activity dew point meter, with temperature control. Brine samples were collected for ionic composition, dissolved organic carbon (DOC), water isotopic composition, and dissolved inorganic carbon (DIC). Samples for ionic composition were analyzed by ACZ labs in Steamboat Springs, CO. A subset of redox sensitive ions ($\sum S^{2-}$, Fe^{++}, NO^{-}_{3}, NH^{+}_{4}) were measured in the field using a Hach Spectrophotometer via established protocols (Osburn *et al*., 2014). DOC was quantified by Anatek labs in Spokane, WA.

Cells were filtered from water for lipid analysis through 90 mm pre-combusted 0.3 µm glass fiber filters using a field peristaltic pump (Geotech). Filters were wrapped in pre-combusted foil and frozen until analysis. In winter 2019 samples of lake ice were also collected by melting ice chunks in cleaned buckets then filtered as described above. Salt and sediments for lipid extraction were collected using solvent-rinsed tools into pre-combusted soil jars from multiple places in each lake or brine pool. Surface sediment samples included only the top 3 cm of sediment. All samples for lipid analysis were frozen within 6 hours of collection, transported frozen to the lab, and stored at -20ºC until further processing.

3.2 Total Organic Carbon and Stable Isotope Analysis

The stable isotopic composition of bulk organic carbon, as well as TOC and TN concentrations were measured in the Northwestern Stable Isotope Biogeochemistry Lab with an elemental analyzer isotope ratio mass spectrometer (EA-IRMS; Costech 4010 EA coupled to a Thermo Delta V+ IRMS through a Conflo IV interface). Lyophilized samples were weighed then were treated with 1M HCl to remove inorganic carbon and acid soluble salts, rinsed with MilliQ water, then lyophilized and weighed again. Thehomogenized sample was loaded into tin capsules for analysis. Standards were run every 10 samples including IU-acetanilide ($\delta^{13}C$ = -29.5 ‰, $\delta^{15}N$ = 1.2 ‰) and urea ($\delta^{13}C$ = -8.0 ‰, $\delta^{15}N$ = 20.2 ‰). Carbon isotopes are reported with respect to Vienna Pee Dee Belemnite (VPDB) and nitrogen isotopes are reported with respect to atmospheric N_2 (AIR; Schimmelmann *et al*. 2009)

3.3 Lipid Extraction

Frozen samples were freeze-dried and homogenized using a solvent-rinsed mortar and pestle. Lipids were extracted from each sample using a modified Bligh and Dyer (Bligh & Dyer, 1959) method according to Johnson *et al*. (2018). In brief, three to six grams of homogenized sample was sonicated with a single-phase mixture of methanol (MeOH), dichloromethane (DCM), and aqueous buffer (2X 50 mM dibasic potassium phosphate, 2X trichloroacetic acid) mixture, centrifuged, and combined. Additional DCM and water were added to form a two-phase solution of which the organic fraction was collected. Elemental sulfur was removed from the lipid extracts by reaction with activated and triple solvent-rinsed copper granules. Samples were then split for ester-bound lipid analysis and ether-bound lipid analysis. Ester-bound lipids were liberated by base saponification with 0.5 M NaOH heated at 70ºC for 16 hours. Saponification reactions were acidified, then the organic fraction was extracted with 10 mL of methyl tert-butyl ether 3 times and dried. To liberate ether-bound core lipids, the method described by Kaneko *et al*. (2011) was employed. In brief, 0.5 mL of hydroiodic (HI) acid was added to dry lipid extracts, purged with a stream of N_2 gas, and heated at 120ºC for 4 hours. Once cooled, 1 ml of clean water and 2 mL hexane were added to the HI and shaken vigorously to extract the cleaved products.

3.4 Lipid Separation and Derivatization

Hydrolyzed ester-bound lipids were separated into four fractions: alkane (4 mL of hexane), ketone (7 mL of 4:1 hexane:DCM), alcohol (7 mL of 9:1 DCM:acetone), and fatty acid (8 mL of 2.5% formic acid in DCM) with aminopropyl substituted solid-phase extraction columns (Supelco, Discovery DSC-NH_2). Alcohol fractions were derivatized to acetate esters with pyridine and acetic anhydride, heated at 70ºC for 20 minutes. Fatty acids were derivatized to methyl esters (FAMEs) with 12.5% Boron Trifluoride (BF_3) in anhydrous MeOH and heated at 70ºC for 10 minutes, followed by extraction with hexane (3x) and removal of water with Na_2SO_4. Cleaved ether lipids were subjected to a hydrogenation reaction to reduce alkyl iodides. The cleaved ether products combined with 5 mg of platinum oxide (PtO_2) under a stream of H_2 gas and stirred between 800 and 1000 rpm for 90 minutes. Data from hydrocarbon, fatty acid, and ether cleavage fractions are discussed here.

3.5 Biomarker Quantification and Identification

Biomarkers were identified and quantified using gas chromatography-flame ionization detection-mass spectrometry (GC-FID/MS) with a ThermoFisher Trace GC 1310 coupled to an FID and ISQ quadrupole MS. A Zebron ZB-5 capillary GC column (30 m × 0.25 mm × 25 μm) was used to separate ester-bound compounds with He carrier gas at 10ml/min. For each ester cleavage sample run, 2 μL was injected into a PTV injector (70ºC initial, evaporated at 100ºC for 1 min, ramped to 320ºC at 10ºC/min?, cleaning at 350ºC). The GC oven temperature schedule for ester-bound lipids was as follows: 1 minute hold at 100ºC, ramped to 320ºC at 14ºC/min, followed by a final 10 minute hold. The MS conditions included ion scanning between 60-600 (amu) every 0.2 seconds. Sample peaks were quantified relative to the intensity of a known quantity of palmitic acid isobutyl ester (PAIBE) added to each sample prior to analysis.

A Zebron ZB-5HT Inferno capillary GC column (30 m × 0.25 mm × 0.25 μm) was used to separate ether-bound compounds with He carrier gas at 10ml/min. For each sample run, 2 μL was injected into a PTV injector (365ºC initial, evaporated at 100ºC for 1 min, ramped to 320ºC at 10ºC/sec, cleaning at 350ºC). The GC oven temperature schedule for ether-bound lipids was as follows: Initial temperature at 70ºC, ramped to 130ºC at 30ºC/min, followed by a ramp to 320ºC at 10ºC/min, and then followed by a final ramp to 350ºC at 8ºC/min. The MS conditions were the same as above.

3.6 Statistical Analyses and Data Visualization

Statistical analyses were performed to evaluate relationships between samples using the 'vegan' package in R (Oksanen *et al*., 2019). Non-metric multi-dimensional scaling (NMDS) with a Bray-Curtis dissimilarity was used to rank the compositional dissimilarity between sites based on differences in abundance and diversity of lipids. Similarly, hierarchical clustering was performed using the linkage library in Python to create a dendrogram of sites based on lipid distributions using the Ward clustering algorithm. All data was visualized using the ggplot2 package in R (Wickham, 2016) or matplotlib in Python (Hunter, 2007).

4. Results

4.1 Brine Geochemistry

The salinity of the brines ranged from 98 ppt to 327 ppt (9.8 to 32.7% salinity). During our study, we encountered the highest salinities during the summer 2019 season from the brine pools

within Basque Lake #1 and Basque Lake #4 showed the highest salinity. The ionic strength of the brines in this study were also exceptionally high ranging from 2.97 to 10.57 (Table 2). Additionally, the water activities of the brines ranged from 0.90 to 0.99. Salt Lake (which did not exhibit distinct brine pools) and one brine pool (Brine 23) within Basque Lake #2 had the lowest measured salinities. Water activities for the brines ranged from 0.90 to 0.99. The lowest water activities were from the sub brine pools within Basque Lake #2 and the highest was from Salt Lake. The pH of all lakes was circumneutral to alkaline. The average pH of each site were as follows: Salt Lake, 8.11; Basque Lake #1, 7.86; Basque Lake #2, 8.39; Basque Lake #4, 7.62; and Last Chance Lake, 9.94 (Table 1).

Table 1. Average Geochemistry of the Brines. Concentrations of ions are reported in g/L. Salinity is reported in parts per thousand (ppt).

Lake	Ca	Mg	Na	Cl	SO_4	CO_3	HCO_3	pH	Salinity	Ionic Strength	a_w
Basque Lake #1											
Brine 1	0.32	59.35	17.20	1.59	242.50	0.00	1.41	7.92	322.35	10.36	0.91
Brine 2	0.33	61.60	16.50	1.54	244.00	0.22	2.54	7.80	326.70	10.57	0.90
Basque Lake #2											
Brine 1	0.35	40.15	17.90	1.63	198.00	0.00	1.94	8.42	259.65	7.87	0.91
Brine 2	0.36	45.20	19.05	1.51	212.00	0.00	1.17	8.45	279.04	8.60	0.90
Brine 3	0.48	30.50	16.65	0.79	141.20	0.06	1.09	8.29	190.29	5.86	0.98
Brine 4	0.38	39.80	15.40	1.55	173.00	0.38	0.23	ND	230.70	7.27	0.93
Brine 23	0.47	15.50	10.20	1.05	83.00	0.25	0.19	ND	110.70	3.27	0.98
Basque Lake #4											
Brine 1	0.48	49.00	27.30	0.69	221.00	0.00	1.27	7.62	299.70	9.27	0.98
Salt Lake											
Brine 1	0.13	14.80	8.86	0.72	73.40	0.22	0.98	8.11	98.13	2.97	0.99
Last Chance Lake											
Brine 1	0.00	0.05	53.60	5.71	18.90	82.30	12.40	ND	160.56	4.49	ND
Brine 4	0.00	0.02	51.20	4.15	13.50	78.40	12.40	9.99	159.70	4.17	0.96
Brine 5	0.01	0.07	82.10	6.97	22.90	62.80	17.60	9.89	192.40	4.60	0.93

*ND values represent lakes for which measurements were not determined.

The dominant cations observed here were Mg^{2+} in the Basque Lakes and Salt Lake and Na^{+} in Last Chance Lake. The dominant anions observed were SO_4^{2-} in the Basque Lakes and Salt Lake with Last Chance Lake dominated by HCO_3^{-} and CO_3^{2-}.

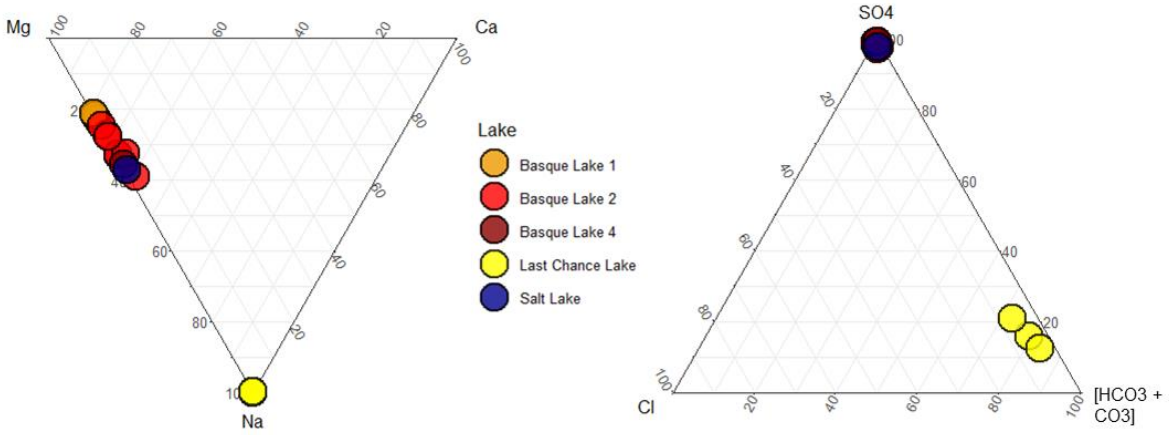

Figure 2. Major ion geochemistry of lake water. Ternary diagrams of the molar fraction of the major cations (*left*) and major anions (*right*).

4.2 Sediment Geochemistry

Bulk OM concentrations in fluids (measured as mg/mL filtered) and solids (mg/g dry weight) varied between the lakes as well as the sample types (Table 2). TOC for all lakes and sample types ranged from at or below detection limit to 42.8%. The $\delta^{13}C$ values of this organic material ranged from -28.3 to -10.2‰. TN ranged from at or below detection limit to 0.3%. $\delta^{15}N$ values ranged from 1.2 to 14.8‰. Total lipid extract (TLE) concentrations determined gravimetrically ranged from 0.21 to 15.70 mg/g dry sample weight. TLE/TOC, representing the proportion of solvent extractable compounds within the total organic carbon, ranged from at or below detection limit to 55.0 mg TLE per g of organic carbon.

Table 2. Measured values for bulk organic matter. Total Lipid Extract (TLE), Total Organic Carbon (TOC), Total Nitrogen (TN).

Season	Brine Pool	Type	TLE	TOC (%)	TN (%)	TLE/TOC	$\delta^{13}C$ (VPDB)	$\delta^{15}N$ (AIR)
Basque Lake #1								
Summer	BL1-1	Mat	7.8	12.3	BDL	0.6	-12.7	BDL
Summer	BL1-1	Salt	0.6	42.8	BDL	0.0	-16.6	BDL
Summer	BL1-1	Sediment	6.7	8.8	BDL	0.8	-18.1	BDL
Summer	BL1-2	Brine	2.6	0.5	BDL	5.7	-22.2	BDL
Summer	BL1-2	Mat	7.0	16.5	BDL	0.4	-16.9	BDL
Basque Lake #2								
Winter	BL2	Brine	2.1	0.1	0.0	15.4	-21.0	6.9
Winter	BL2	Ice	3.9	0.1	0.0	25.9	-22.0	7.3
Winter	BL2	Salt	1.0	0.3	0.0	7.9	-16.7	8.6
Winter	BL2	Sediment	6.2	1.2	0.1	9.3	-18.2	9.4
Summer	BL2-1	Brine	2.5	1.0	BDL	2.6	-17.8	BDL
Summer	BL2-1	Sediment	7.9	1.7	0.2	7.3	-18.8	8.5
Summer	BL2-11	Mat	15.7	BDL	BDL	BDL	BDL	BDL
Summer	BL2-2	Brine	1.3	0.9	BDL	1.5	-15.1	BDL
Summer	BL2-23	Brine	1.9	0.9	BDL	2.3	-17.6	BDL
Summer	BL2-23	Mat	10.3	23.1	BDL	0.4	-15.1	BDL
Summer	BL2-23	Salt	2.7	BDL	BDL	BDL	BDL	BDL
Summer	BL2-23	Sediment	6.4	12.5	BDL	0.5	-13.1	BDL
Summer	BL2-3	Brine	4.8	BDL	BDL	BDL	BDL	BDL
Summer	BL2-3	Salt	0.4	BDL	BDL	BDL	BDL	BDL
Summer	BL2-3	Sediment	6.5	0.7	0.1	31.7	-16.1	7.7
Summer	BL2-4	Brine	3.1	1.0	BDL	3.0	-19.8	BDL
Summer	BL2-41b	Sediment	6.3	BDL	BDL	BDL	BDL	BDL
Summer	BL2-44b	Mat	3.3	BDL	BDL	BDL	BDL	BDL
Basque Lake #4								
Summer	BL4	Brine	1.1	0.3	BDL	3.5	-20.3	BDL
Summer	BL4	Salt	0.3	BDL	BDL	BDL	BDL	BDL
Summer	BL4	Sediment	5.9	9.7	BDL	0.6	-17.5	BDL
Last Chance Lake								
Winter	LCL1	Brine	0.6	0.1	0.0	10.4	-28.3	5.1
Winter	LCL1	Ice	5.3	0.1	0.0	55.0	-27.6	6.3
Winter	LCL1	Salt	0.2	0.3	0.0	0.6	-22.8	5.1
Summer	LCL1	Sediment	3.0	0.8	0.0	5.1	-24.8	10.7
Summer	LCL1	Mat	5.2	2.3	0.2	40.7	-23.2	12.2
Summer	LCL4	Brine	1.0	0.8	BDL	1.3	-25.2	BDL
Summer	LCL4	Mat	8.5	2.6	BDL	3.2	-26.4	BDL
Summer	LCL4	Sediment	1.3	1.4	BDL	1.0	-24.3	BDL
Summer	LCL5	Brine	1.1	0.3	BDL	3.8	-25.7	BDL
Summer	LCL5	Mat	3.2	0.9	BDL	3.3	-25.5	BDL
Summer	LCL5	Sediment	1.6	0.9	BDL	1.7	-24.3	BDL
Salt Lake								
Winter	SL	Brine	0.8	0.1	0.0	18.8	-24.6	3.1
Winter	SL	Ice	2.6	0.1	0.0	28.2	-28.3	6.9
Winter	SL	Salt	0.5	0.1	0.0	4.4	-23.9	7.5
Winter	SL	Sediment	8.1	0.5	0.1	19.1	-21.8	6.6
Summer	SL1	Brine	3.2	BDL	BDL	BDL	BDL	BDL
Summer	SL1	Salt	0.2	0.0	0.0	6.8	-20.8	9.9
Summer	SL1	Sediment	3.3	2.5	0.3	1.7	-21.2	9.0

*BDL (below detection limit) values represent lakes for which samples measurements could not be determined due to sample material limitations.

On average, Basque Lake #1 had the highest TOC (mean 16.63%) and Salt Lake the lowest (mean 0.79%) with Basque Lake #2, Basque Lake #4, and Last Chance Lake falling intermediate. Microbial mats and sediments had higher TOC than salts and brines with the exception of salt dissolution residues from Basque Lake #1 and brines from Last Chance Lake. The average ratio between TOC in the sediment ($TOC_{sediment}$) relative to TOC in the brine (TOC_{brine}) is used to normalize the sedimentary accumulation of OM to that produced in the water column between lakes. These calculations showed that Mg-SO_4 dominated lakes had high $TOC_{sediment}/TOC_{brine}$ ratios (average 20.7) compared to the Na-CO_3 lake (average 2.8) (Fig. 3F). The carbon isotopic composition of bulk organic matter varied considerably between lakes with the most ^{13}C-enriched values deriving from Basque Lake #1 (mean -16.6‰) and the most ^{13}C-depleted from Last Chance Lake (mean -24.8‰) (Fig. 3D). These values also varied by sample type with the most ^{13}C-enriched values deriving from the sediments and most ^{13}C-depleted from the brines.

The concentration of total nitrogen (TN) and its isotopic composition varied within and between lakes (Fig. 3B) but was often at or below the level of detection with our methods. Samples from Basque Lake #2, Last Chance Lake, and Salt Lake had TN values that spanned a relatively large range from below the limit of detection to 0.3% N. Basque Lake #1 and #4 yielded very small amounts of TN, typically less than what is required for analysis. The isotopic composition of nitrogen ($\delta^{15}N_{TN}$), where measurable, also varied widely between and within lakes exhibiting more ^{15}N-enriched average values in LCL, intermediate values in the Basque lakes, and more ^{15}N-depleted values in Salt Lake (Fig. 3E)

The yields of extractable lipids (TLE) showed similar mean values between lakes but large distributions (Fig. 3C). Mean TLE concentrations ranged from 2.42 mg to 5.11 mg per gram of sediment and varies systematically by sample type. Generally, the sediments and microbial mats have the highest TLE in all lakes except Last Chance Lake where brine (in mg/L) is the highest. Conversely, the salt samples consistently had the lowest concentrations of TLE in all lakes. The TLE concentrations for brines typically fell between sediments and salts.

To estimate the production of lipids with respect to OM, we calculated the relative proportion of total lipids relative to organic matter (TLE/TOC) for each sample (Figure 3F). The

highest mean ratios of TLE/TOC are found in salts with the exception of Salt Lake and Basque Lake #4. Additionally, within individual lakes, brines generally have a higher TLE/TOC ratio (representing a higher relative lipid contribution) than sediments except for Basque Lake #2 which shows a higher proportion of TLE/TOC in the sediments relative to the brines. Including all sample types, Basque Lake #1 recorded the highest ratios of TLE/TOC (14.12) whereas Basque Lake #4 recorded the lowest average ratio (2.07).

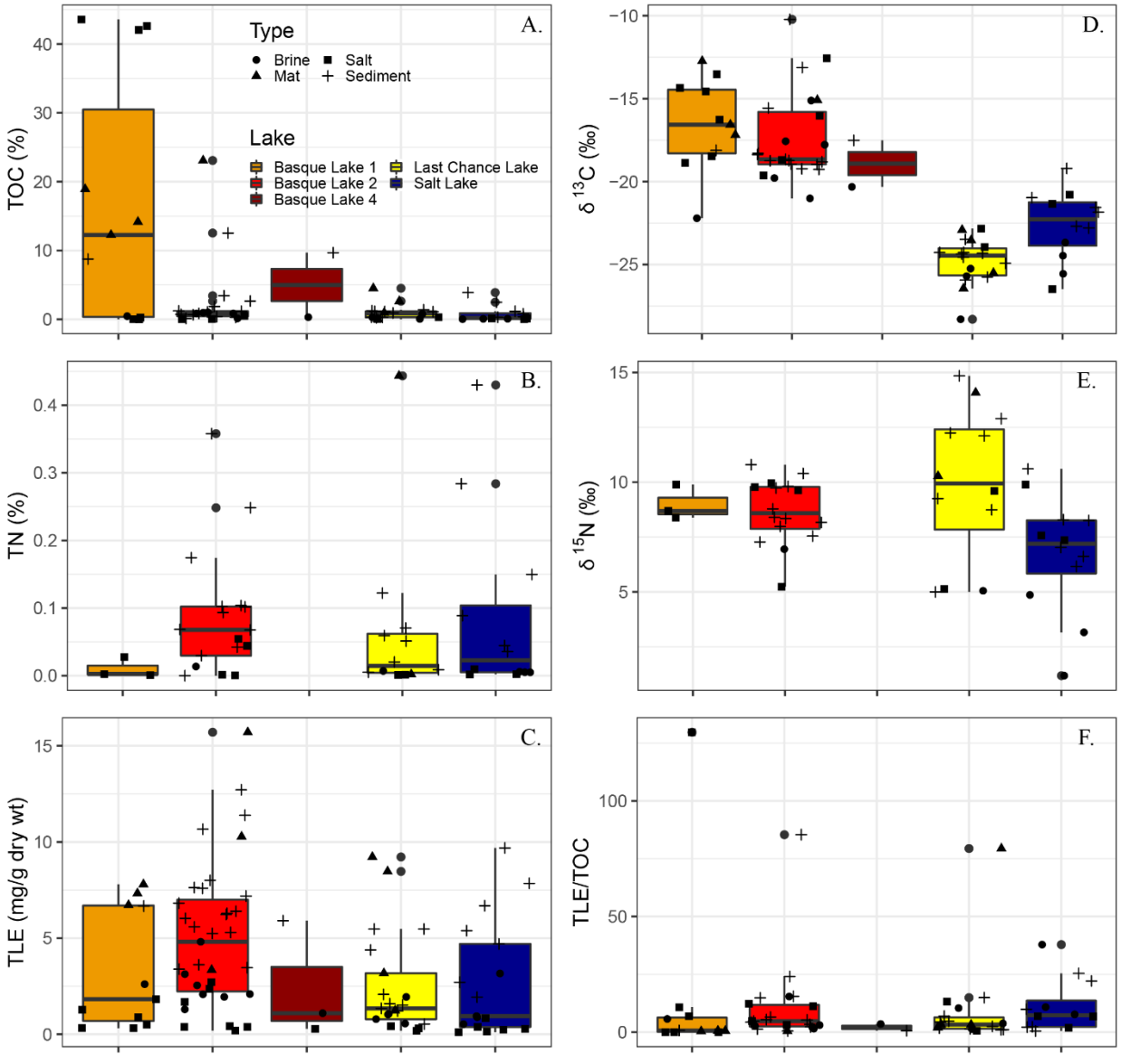

Figure 3. Box and whisker plot of bulk organic matter parameters. A. Total Organic Carbon Abundance, B. Total Nitrogen Abundance, C. Total Lipid Extract, D. $\delta^{13}C$ Isotopic Composition

of Organic Matter, E. $\delta^{15}N$ Isotopic Composition of Samples, F. Lipid Production as mg of TLE with respect to g of Organic Carbon.

4.3 Lipid Composition and Distribution

We detected a variety of lipid compounds in all sample types including fatty acids, alkanes, and ether-bound lipids. Fatty acids were more abundant than alkanes in the ester-cleaved fractions. Alkanes were measured but are minor contributors (<5%) to the lipid distribution in the mat, brine, and salt samples, although they do comprise a moderate proportion (~10-20%) in sediment samples. Similarly, ether-bound lipids constitute a very minor proportion (<1%) of the total lipids recovered from these samples, although this may be due to a known problem of low yields of this method (Kaneko et al., 2011).

Sediments and mat sample contained the greatest diversity of fatty acids, with 54 unique compounds present. The distribution of fatty acids is broadly similar across sample types and sites with a few notable exceptions: (which are?). Brine samples consistently contained primarily short saturated and monounsaturated fatty acids (MUFAs). Sediment samples show the greatest diversity of lipids across sites and include an abundance of long saturated and branched fatty acids. The sediments also show a decrease in the proportion of MUFAs relative to short saturated compounds. The most abundant fatty acids in our samples were *n*-C16:0, C16:1, C16:2, *n*-C18:0, and C18:1; however, the carbon chain lengths present ranged from C12 to C32. The *i*-C14:0, *i*-C15:0, *a*-C15:0, and *a*-C16:0, and *i*-C17:0 branched fatty acids are also present in many samples with *i*-C15:0 and *a*-C15:0 being the most abundant. The *i*-C17:0, *a*-C16:0 and *i*-C14:0 are relatively abundant with the latter predominantly present only in the sediments. Across all sample types, there is an even-over-odd preference in the fatty acid distribution. This is especially apparent in the brines and mats where only even-chain fatty acids are present above carbon chain length 18, with the exception of three mat samples that contained a very low abundance of *n*-C23:0 and *n*-C25:0. The long chain saturated fatty acids from the sediments also show this pattern although odd-chain fatty acids are present. We identified both isoprenoidal and alkyl products from cleavage of ether-bound lipids. The primary isoprenoidal ether-bound lipid identified was phytane (*iso*-C20) whereas the primary alkyl product was *n*-C16 and *n*-C18. Ether-bound lipids, including both isoprenoidal and alkyl, were most abundant in Last Chance Lake.

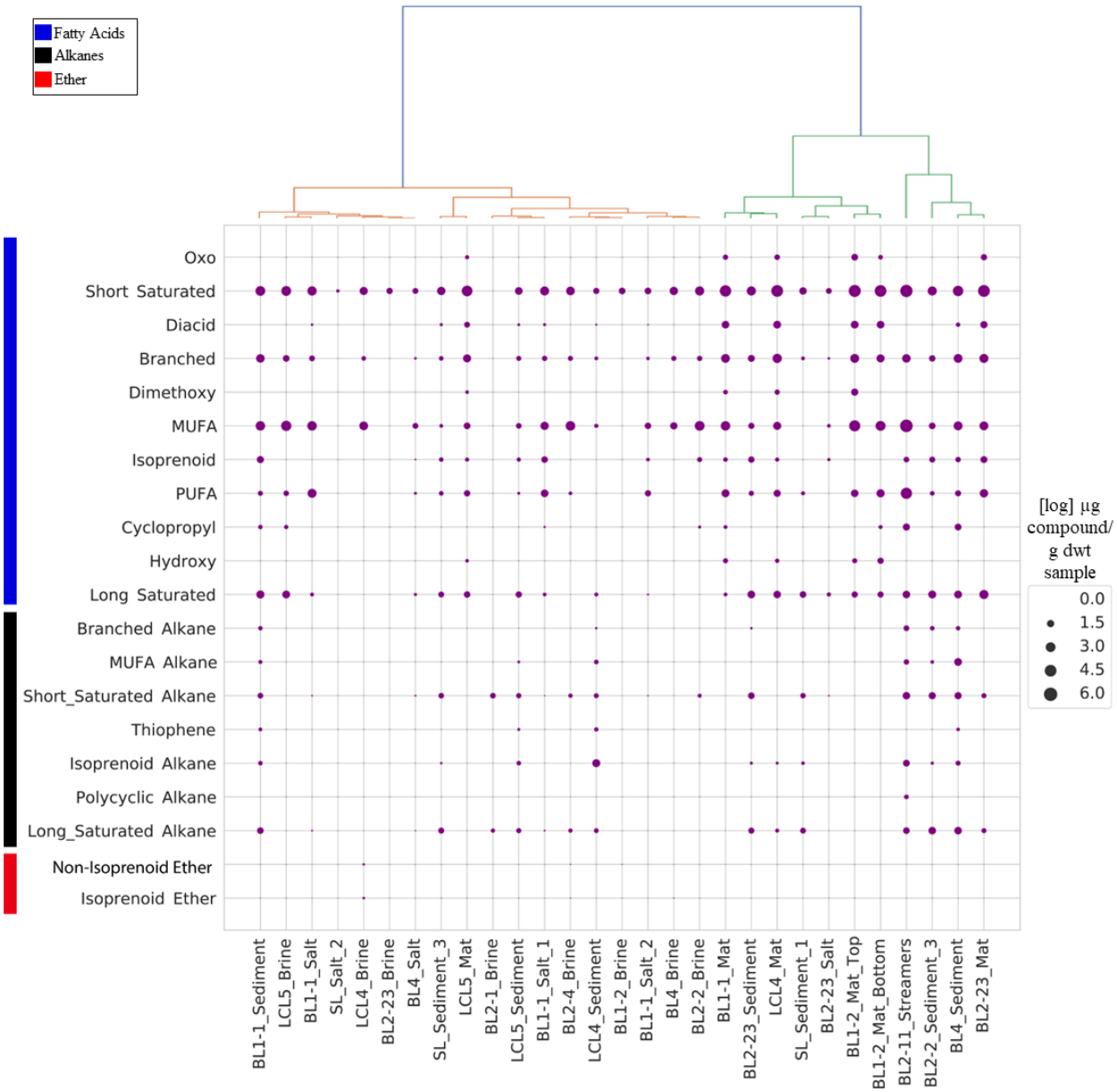

Figure 4. **Lipid composition and abundance.** Summed concentrations of lipid classes are represented with respect to samples. Bubble size represents log concentration of µg compound/g sample dry weight (dwt). Samples are arranged based on hierarchical clustering using Ward's method. The orange and green colors of the dendrogram represent the two distinct clusters within our samples. The blue bar indicates fatty acids, the black bar indicates alkanes, and the red bar indicates ether-bound lipids.

5. Discussion

5.3 Lipid Biomarker Production and Preservation

Lipid biomarkers are quantifiable and provide taxonomic specificity to the domain, and sometimes finer levels, which allow for a differentiation of lipid sources (Willers *et al*., 2015). Bacteria typically contain membranes composited of diacyl glycerides where fatty acids are ester-linked to glycerol backbones with a range of polar head groups (Willers *et al*., 2015). In these membranes fatty acid moieties are typically 14-22 carbons long, including mono- and dialkenes, and branches, or cyclopropyl rings (Sohlenkamp & Geiger, 2016; Willers *et al*., 2015). While less typical, some bacteria are also able to synthesize ether-bound lipids with alkyl chains usually 15 or 16 carbons long (Bale *et al*., 2021; Grossi *et al*., 2015). Terrestrial plants produce leaf waxes composed of fatty acids and *n*-alkanes generally dominated by carbon chain lengths ranging from 25-31 (Bush & McInerney, 2013; Diefendorf, 2011). Archaea synthesize ether-linked isoprenoidal lipid membranes with either diethers, tetraethers, or a combination and can feature a variety of rings and hydroxyl group modifications (Schouten *et al*., 2012).

Different lipid classes also show varying reactivities towards microbially mediated processes and therefore certain classes have a potential for long term preservation. However, the relative lability of lipids is also dependent on local depositional conditions, including temperature, oxidation state, and importantly, salinity (Schouten *et al*., 2010; Sun *et al*., 1997; Canuel & Martens, 1996; Middleburg *et al*., 1989; Harvey *et al*., 1986). For instance, studies have shown that under oxic conditions, lipids degrade more quickly than under otherwise similar anoxic ones (Sun *et al*., 1997; Canuel & Martens, 1996). Fatty acids are generally more labile than alkanes, thus, in sedimentary systems they can represent either an active microbial community or well preserved organic matter. Conversely, alkanes are more refractory and often by-products of degradation reactions or plant material, ultimately, recording a terrestrial or past community. Ether-linkages in lipids are very stable and thus ether lipids are well preserved in the geologic record (Schouten *et al.*, 2013).

The biosignature profiles found in the BC lakes across all sample types suggest that *in situ* microbial biomass (indicated by short chain, saturated and unsaturated, fatty acids), rather than plant-based allochthonous material (long chain alkanes and fatty acids) is the dominant source of OM in these systems, despite the heavily vegetated watersheds. This conclusion is supported by relative dominance of monounsaturated lipids (>50% relative abundance) in brines and sediments, (Willers *et al*., 2015). Surface sediments show elevated concentrations of long saturated fatty acids (> 5% relative abundance) and long chain alkanes with respect to the overlying brine (< 5% relative

abundance), showing the incorporation and selective preservation of material from surrounding vegetation; however, the dominant biosignature remains microbial. Further, branched fatty acids, which are produced exclusively by bacteria, are found in elevated concentrations in microbial mat and sediment samples. The presence of the terminally branched fatty acids *i*-C15, *a*-C15, and *i*-C17 in the hypersaline lakes is often attributed to the presence of sulfate reducing bacteria (SRB; Perry *et al*. 1979; Tan *et al*., 2018). Given the high concentrations of SO_4 in our lakes and sulfide in the sediments, this origin is likely. The increased abundance of branched fatty acids in the sediments compared to the brines, specifically *a*-C15 further suggests the role of SRB as these anaerobes will increase in abundance in anoxic settings (Tan *et al.*, 2018). Moreover, the presence and abundance of the MUFAs C16:1 and C18:1 within the brines is consistent with the lipids produced by cyanobacteria or algae as well as many other bacteria (Willers *et al*., 2015). As bulk $\delta^{13}C$ values of organic matter in these samples are more ^{13}C-enriched than expected for lacustrine algae and the abundance of polyunsaturated compounds is low, we suggest that cyanobacteria are the dominant source for these unsaturated fatty acids.

The dominance of short-chain fatty acids as opposed to long-chain fatty acids and alkane biomarkers indicates that an extant microbial community is producing lipids which are well preserved as they are incorporated into the sedimentary record. This distribution is in contrast to that found at other Martian analog systems such as the acidic SO_4- rich hypersaline lakes in Western Australia which show a greater proportion of alkanes and long-chain fatty acids. Additionally, ether-bound lipids are in low abundance relative to ester-bound lipids and include isoprenoidal (archaeal-derived) and non-isoprenoidal (bacterial-derived), which suggests a dominantly bacterial rather than archaeal biomarker signature. Our observation of minor archaeal lipid inputs is consistent with the metagenomic analysis presented by Pontefract *et al*., (2017) of a nearby SO_4-rich hypersaline lake which found only minor contributions of archaea to the microbial community (amplicon and metagenomic sequence data for these lakes is forthcoming, Pontefract et al., *in prep*). The low concentrations of Na^+ in our study sites may be responsible for the minor archaeal lipid inputs as studies have shown that halophilic archaea require a minimum NaCl concentration of 1.5 M (Mesbah & Wiegel, 2008; Robinson *et al*., 2005). This is consistent with our results as the only lake with elevated archaeal lipid concentrations was the Na-CO_3 dominated lake.

5.2 Sample Variation of Lipid Composition

A key motivating question of this study is how kosmotropic and chaotropic ions change biosignature production and preservation and how this varies across chemical gradients within hypersaline systems. To reduce the inherent complexity in environmental samples and their chemical compositions, we performed a non-metric multidimensional scaling (NMDS). This analysis allows us to discern the dominant controls on the variation across and between samples. While the lakes varied spatially and chemically, the NMDS analysis shows that the lipid distribution is most influenced by sample type (Figure 5). Brine and salt samples were most similar to each other in this ordination, and sediment and mat samples also trended together. The link between brines and salts could suggest that microbes aid in the formation and precipitation of salts either by providing a nucleation site or by promoting precipitation through metabolic activities (Cabestrero *et al*., 2018). Alternatively, material from the brine could be simply trapped within precipitating salts (Cabestrero *et al*., 2018). The sampled microbial mats were benthic, likely incorporating some surface sediments, which explains the similarity in lipid composition between these and sediment samples. Additionally, the abundance of alkanes differentiates the sediment samples from all other sample types as shown by the computed eigenvectors. In contrast, brines and salt sample types are differentiated by their high concentrations of monounsaturated and polyunsaturated fatty acids (Figure 5). These data suggest that the primary mechanism controlling the lipid distributions in these lakes are factors shared between lakes (notably not chemical composition) including sediment morphology, sedimentation rate, or mean annual temperature.

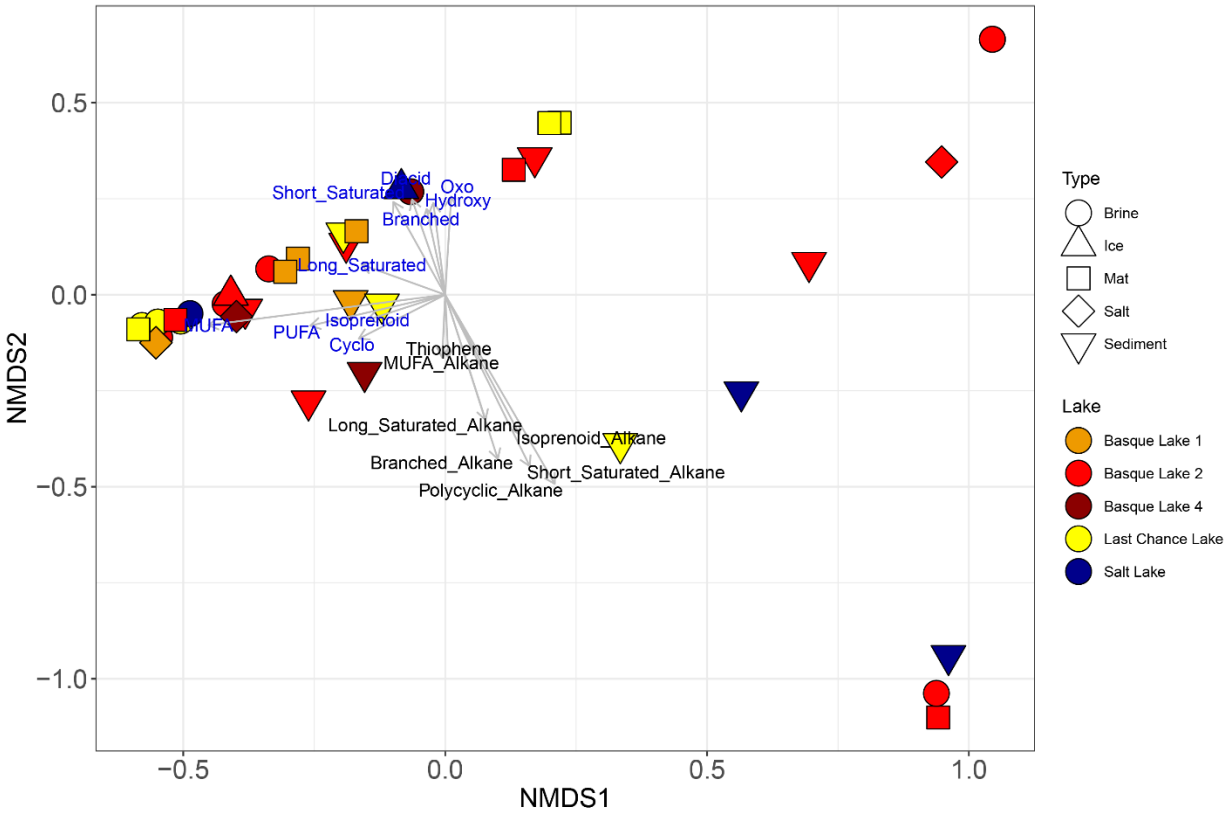

Figure 5. A non-metric multidimensional scale (NMDS) of our samples. Distances were calculated using the Bray-Curtis metric. Stress = 0.018. Vectors were computed for compounds that contributed variance on the samples with p values less than 0.01. Blue labels represent fatty acid compounds whereas black labels represent alkanes.

5.3 Bulk Organic Matter Abundances and Isotopic Values

Bulk organic parameters such as TOC, TN, and $\delta^{13}C_{TOC}$ values integrate both biomass production and degree of degradation (Meyers, 2003) and can be used to constrain the sources of biomass in lacustrine systems (i.e. land-derived or aquatic-derived) (Meyers, 2003; Meyers; 1994). For instance, OM from algae tends to be protein-rich producing a C/N ratio between four and ten (Meyers, 2003; Meyers, 1994), whereas vascular plant biomass is protein-poor but cellulose rich, producing high C/N ratios reaching values of 20 or greater (Meyers, 2003; Meyers, 1994). $\delta^{13}C_{TOC}$ values provide complementary information reflecting the mechanisms of carbon fixation and assimilation (Meyers, 2003; Hayes, 2001).

Bulk organic measurements described here provide further evidence that the primary biosignature is of *in situ* microbial origin rather than exogenous material (Figure 6). Data from the SO_4-dominated lakes, Basque Lake and Salt Lake, group together with low C/N and ^{13}C-enriched isotope values consistent with a microbial source. In contrast, the CO_3-dominated lake, Last Chance Lake, shows ^{13}C-depleted OM that ranges to very high C/N values. This overall pattern of ^{13}C-depleted OM and high C/N values suggests a mixed OM signal resulting from either exogenous input or a higher degree of degradation (Meyers, 1994).

To differentiate between production potential and degree of degradation, we calculated $TOC_{sediment}/TOC_{brine}$ ratios. The Mg-SO_4 lakes have the highest values with respect to the CO_3^- dominated lake, suggesting a slower rate of organic carbon remineralization within the Mg-SO_4 lakes, ultimately, leading to an increase in the concentration of TOC in the sediment with respect to what is produced in the brine. These results agree with the bulk isotope data. Alternatively, this higher ratio might could be driven in part by a productive anaerobic community in the surface sediments or high mineral surface areas of the sediments. Elevated concentrations of the branched fatty acids *i*-C15, *a*-C15, and *i*-C17 in the sediments of these lakes support this mechanism.

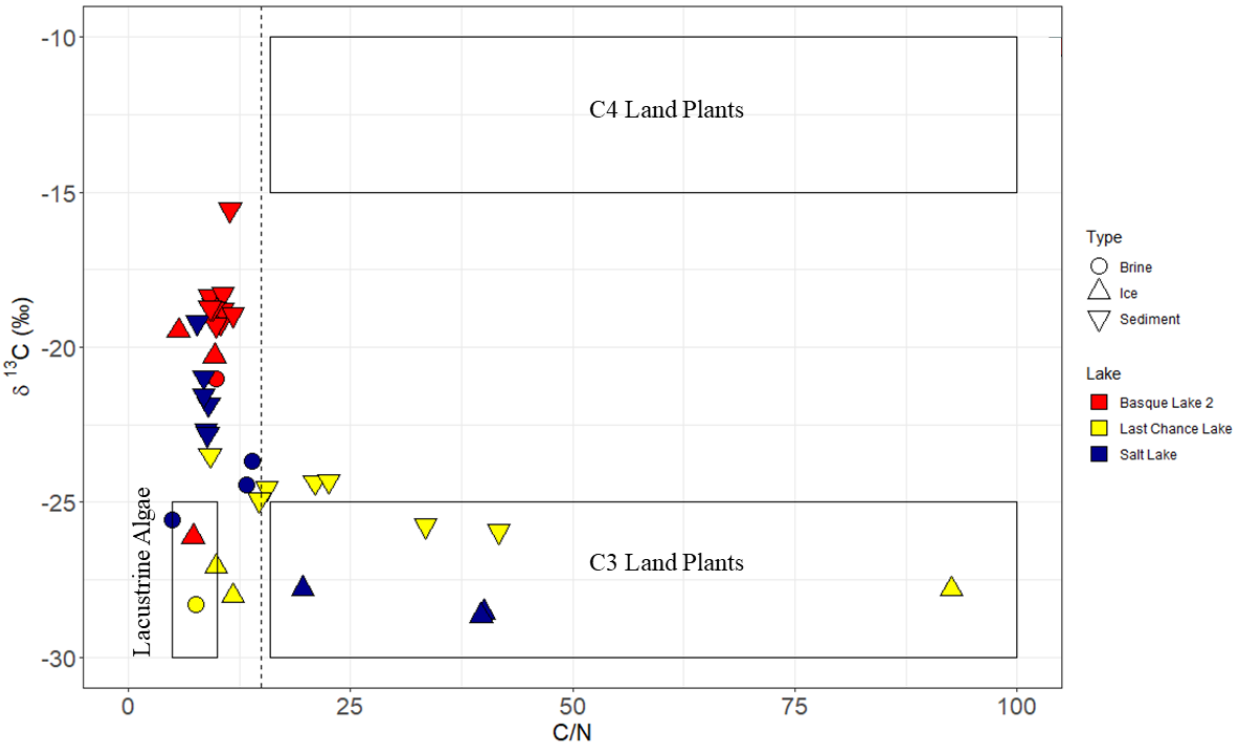

Figure 6. Cross-plot showing the relationship between C/N ratio and bulk carbon isotopic composition of OM. The dashed line indicates the typical cutoff for an aquatic vs terrestrial signature of 15 (Meyers, 1994) and boxes represent the general composition for C_4 and C_3 land plants.

5.4 Sulfate-Rich Lakes

Most hypersaline systems on Earth are dominated by NaCl with the Cl^- anion being chaotropic or membrane destabilizing (Pontefract *et al*., 2017; Hallsworth *et al*., 2007). As such, many hypersaline lakes investigated as Mars analogs are Cl-dominated. These sites such as Don Juan Pond ($CaCl_2$) in Antarctica, the Discovery Basin ($MgCl_2$) in the Mediterranean, and the South Bay Salt Work Bitterns (NaCl and $MgCl_2$ gradient) in Southern California are some of the lowest biomass places on Earth, with both low microbial diversity and preservation of organic material (Klempay *et al*., 2021; Dickson *et al*., 2013; Hallsworth *et al*., 2007). This begs the question for the production and preservation of lipid biomarkers in other aqueous solutions of varying kosmotropic or membrane stabilizing settings.

Extremely SO_4-rich aqueous environments are rare on Earth but are known from geographic regions like South-Central British Columbia and Western Australia (Johnson *et al*., 2020; Pontefract *et al*., 2017). Previous biosignature work on these Mars-analog environments has shown a range of OM production, preservation, or microbial activity. Work done using metagenomic analysis in Spotted Lake (South-Central British, Columbia), a circumneutral Mg-SO_4 lake, found a diverse and abundant microbial community (Pontefract *et al*., 2017). In contrast, lipid biosignature analysis in acidic sulfate-rich lakes (Lake Gneiss and Lake Gilmore, Western Australia) showed very low concentrations of microbial lipids, especially short saturated and branched fatty acids (Johnson *et al*., 2020), which the authors attributed to destruction by the acidic conditions of these Australian lakes. The dominant preserved lipids here were long chain *n*-alkanes and long saturated fatty acids indicating a selective preservation of terrestrial vegetation in that environment.

The lakes described here chemically and physically resemble Spotted Lake and feature similarly abundant microbial biomass. Additionally, the lakes in our study are potentially representative of ancient Martian brines as they show exceptionally both high water activities and high ionic strengths similar to those simulated on ancient Martian surface (Fox-Powell *et al.*,

2016). Yet, despite these ionic strengths, which is thought to be limiting to life, our data shows an abundance of microbially-derived lipid biomarkers. Our results suggest that these circumneutral Mg-SO_4-dominated hypersaline environments feature high OM production and strong preservation potential of lipid biosignatures. This corroborates the work done by Pontefract *et al*., 2017 in Spotted Lake, and is in significant contrast to the Western Australian lakes studied by Johnson *et al.*, 2020 and other Mars analog environments such as Cl-dominated hypersaline systems which have shown low abundance of lipid biosignatures and poor preservation (Klempay *et al.*, 2021; Johnson *et al*., 2020; Dickson *et al.*, 2013; Hallsworth *et al.*, 2007). The implication of this difference suggests that circumneutral Mg-SO_4 dominated hypersaline systems have greater biosignature preservation potential and, ultimately, are better targets for astrobiological investigation than their acidic or Cl-dominated counterparts.

5 Conclusions

We find abundant OM production with biosignatures suggestive of microbial origin within the hypersaline SO_4-dominated lakes of the Cariboo Plateau. These signatures are typical of compounds produced by microbes, specifically sulfate reducing bacteria and cyanobacteria, rather than material derived from surrounding vegetation or archaea. We do observe an increase in lipid diversity, including terrestrially derived material, in sediments indicating selective degradation of the more labile lipids in the water column and selective preservation of the refractory lipids in the sediments. The refractory lipids are likely present in the brines at below detection limit, however, ultimately get concentrated in the sediments due to a lack of remineralization in the brines. Additionally, it is worth noting that the labile lipids detected in the surface sediments likely reflect preservation of those molecules as well as production via benthic mats and sulfate-reducing bacteria within the sediments. Comparison between lake targeted here suggests that Mg-SO_4 dominated environments show greater OM production and preservation of microbial lipid biosignatures than those of other chemistries.

Overall, our study highlights that despite their extreme salinities and ionic strengths, these saturated Mg-SO_4 brines of circumneutral to alkaline pH are teeming with life, producing an abundance of biosignatures. Additionally, despite the Mg^{2+} cation being highly chaotropic, the presence of the compensating kosmotropic anion SO_4^{2-} appears to negate the destabilizing effects of the Mg^{2+} ion. These lipid profiles are distinct from those found in Cl-dominated environments

as bacteria are the dominant lipid-producing microorganisms rather than archaea and algae. Compared to other terrestrial Mars-analog environments these systems show excellent preservation potential for organics, which is directly informative for current and future life-detection missions. While we have demonstrated preservation in the shallowest sediments, future work will target how well these biosignatures are preserved on geologic timescales.

Acknowledgements

This work was supported by a grant from NASA Exobiology to AP and MRO (NNH17ZDA001N-EXO). Drone images were taken by Mitchell Barklage, PhD. MRO is a fellow in the CIFAR Earth 4D program. This work would not have been possible without the aid in sample/data collection from Jacob Buffo, PhD and Emma Brown (Georgia Tech University). All R and Python scripts will be available through GitHub (https://github.com/FloydNichols97/BC_Surface_Dataset).

References

Aubrey, A., Cleaves, H.J., Chalmers, J.H., Skelley, A.M., Mathies, R.A., Grunthaner, F.J., Ehrenfreund, P., and Bada, J.L. (2006). Sulfate Minerals and Organic Compounds on Mars. *Geology* 34(5), 357-360.

Baas, M., Pancost, R., van Geel, B., and Sinnighe Damste, J.S. (2000). A Comparative of Lipids in *Sphagnum* Species. *Organic Geochemistry* 31(6), 535-541.

Bale, N.J., *et al*. (2021). Lipidomics of Environmental Microbial Communities. I: Visualization of Component Distributions Using Untargeted Analysis of High-Resolution Mass Spectrometry Data. *Front. Microbiol.* 12.

Barbieri, R., and Stivaletta, N. (2011). Continental Evaporites and the Search for Evidence for Life on Mars. *Geol. J.* 46, 513-524.

Beadle, L. C. (1974). The Inland Waters of Tropical Africa. Longman, London. 365

Bendia, A.G., Araujo, G.G., Pulschen, A.A., Contro, B., Duarte R.T.D., Rodrigues, F., Galante, D., Pellizari, V.H. (2018). Surviving in Hot and Cold: Psychrophiles and Thermophiles from Deception Island Volcano, Antarctica. *Extremophiles* 22, 917 - 929.

Benison, K.C., and Karmanocky III, F.J. (2014). Could Microorganisms be Preserved in Mars Gypsum? Insights from Terrestrial Examples. *Geology* 42(7), 615-618.

Berner, R.A. (1964). An Idealized Model of Dissolved Sulfate Distribution in Recent Sediments. *Geochim. Cosmo. Acta* 28, 1497-1503.

Bligh, E.G., and Dyer, W.J. (1959). A Rapid Method of Total Lipid Extraction and Purification. *Can. J Biochem Physiol* 37(8), 911-917.

Brocks, J.J., and Pearson, A. (2005). Building the Biomarker Tree of Life. *Reviews in Mineralogy and Geochemistry* 59, 233-258.

Bush, R.T., and McInerney, F.A. (2013). Leaf Wax n-Alkane Distributions in and Across Modern Plants: Implications for Paleoecology and Chemotaxonomy. *Geochimica et Cosmochimica Acta.* 117(15), 161-169.

Cabestrero, O., del Buey, P., and Sanz-Montero, M.E. (2018). Biosedimentary and Geochemical Constraints on the Precipitation of Mineral Crusts in Shallow Sulphate Lakes. *Sedimenary Geology* 366, 32-46.

558 Canuel, E.A., Martens, C.S. (1996). Reactivity of Recently Deposited Organic Matter:
559 Degradation of Lipid Compounds Near the Sediment-Water Interface. *Geochemica and*
560 *Cosmochemica Acta* 60(10), 1793-1806.
561 Carrizo, D., *et al*. (2019). Lipid Biomarker and Carbon Stable Isotope Survey on the Dallol
562 Hydrothermal System in Ethiopia. *Astrobiology* 19(12), 1474 - 1489.
563 Cheng, Z., *et al.* (2017). Bacterial and Archaeal Lipids Recovered from Subsurface Evaporites of
564 Dalangtan Playa on the Tibetan Plateau and Their Astrobiological Implications.
565 Astrobiology.
566 Cui, Y., Miller, D., Schiarizza, P., and Diakow, L.J. (2017). British Columbia digital geology.
567 *British Columbia Ministry of Energy, Mines and Petroleum Resources*, British Columbia
568 Geological Survey Open File 2017-8, 9p. Data version 2019-12-19.
569 Des Marais, D.J., *et al*. (2008). The NASA Astrobiology Roadmap. *Astrobiology* 8(4), 715-730.
570 Dickson, J. L., Head, J. W., Levy, J. S., and Marchant, D. R. (2013). Don Juan Pond, Antarctica:
571 near-surface CaCl(2)-brine feeding Earth's most saline lake and implications for Mars. Sci.
572 Rep. 3:1166
573 Diefendorf, A.F., *et al*. (2011). Production of n-Alkyl lipids in Living Plants and Implications for
574 the Geologic Past. *Geochimica et Cosmochimica Acta*, 75(23), 7472-7485.
575 Ehlmann, B.L.; Mustard, J.F., Murchie, S.L., Poulet, F., Bishop, J.L., Brown, A.J., Calvin., W.M.
576 Clark, R.N., Des Marais, D.J., Milliken, R.E., Roach, L.H., Roush, T.L., Swayze, G.A.,
577 Wray, J.J. (2008). Orbital Identification of Carbonate-Bearing Rocks on Mars. *Science* 322,
578 (5909).
579 Eigenbrode, J.L., Summons, R.E., Steele, A., Freissinet, C., Millan, M., Navarro-Gonzalez, R.,
580 Sutter, B., McAdam, A., Franz, H.B., Glavin, D.P., Arcer Jr., P.D., Mahaffy, P.R., Conrad,
581 P.G., Hurowitz, J.A., Grotzinger, J.P., Gupta, S., Ming, D.W., Sumner, D.Y., Szopa, C.,
582 Malespin, C., Buch, A., and Coll, P. (2018). Organic Matter Preserved in 3-Billion-Year-
583 Old Mudstones at Gale Crater. *Science* 360(6393), 1096-1101.
584 Eugster, H.P., Hardie, L.A. (1978). Saline Lakes. In: Lerman A. (eds) Lakes. Springer, New York,
585 NY.
586 Fox-Powell, M.G. & Cockell, C.S. (2018). Building a Geochemical View of Microbial Salt
587 Tolerance: Halophilic Adaptation of *Marinococcus* in a Natural Magnesium Sulfate Brine.
588 *Front. Microbiol.* 16.

589 Fox-Powell, M.G., *et al*. (2016). Ionic Strength is a Barrier to the Habitability of Mars.
590 *Astrobiology*. 16(6), 427-442.
591 Gock, M.A., *et al*. (2003). Influence of Temperature, Water Activity and pH on Growth of Some
592 Xerophillic Fungi. *International Journal of Food Microbiology* 2481, 11-19.
593 Grant, W.D. (2004). Life at Low Water Activity. *Phil. Trans. R. Soc. Lond.* 359, 1249 - 1267.
594 Grossi, V., Mollex, D., Vincon-Laugier, A., Hakil, F., Pacton, M., and Cravo-Laureau, C. (2015).
595 Mono- and Dialkyl Glycerol Ether Lipids in Anaerobic Bacteria: Biosynthetic Insights
596 from the Mesophilic Sulfate Reducer *Desulfatibacillum alkenivorans* PF2803. *Applied and*
597 *Environmental Microbiology* 81(9), 3157-3168.
598 Grotzinger, J.P., *et al*. (2014). A Habitable Fluvio-Lacustrine Environment at Yellowknife Bay,
599 Gale Crater, Mars. *Science* 343.
600 Hallsworth, J.E., Yakimov, M.M., Golyshin, P.N., Gillion, J.L.M., D'Auria, G., de Lima Alves,
601 F., La Cono, V., Genovese, M., McKew, B.A., Hayes, S.L., Harris, G., Giuliano, L.,
602 Timmis, K.N., and McGenity, T.J. (2007). Limits of Life in $MgCl_2$-Containing
603 Environments: Chaotropicity Defines the Window. *Environmental Microbiology* 9(3), 801
604 - 813.
605 Harvey, H.R., *et al*. (1986). The Effect of Organic Matter and Oxygen on the Degradtion of
606 Bacterial Membrane Lipids in Marine Sediments. *Geochim. Cosmo. Acta* 50, 795-804.
607 Hedges, J.I., Baldock, J.A., Gelinas, Y., Lee, C., Peterson, M., and Wakeham, S. (2001). Evidence
608 for Non-Selective Preservation of Organic Matter in Sinking Marine Particles. *Nature* 409,
609 801-804.
610 Heldmann, J.L., Pollard, W., McKay, C.P., Marinova, M.M., Davila, A., Williams, K.E., Lacelle,
611 D., & Andersen, D.T. (2013). The High Elevation Dry Valleys in Antarctica as Analog
612 Sites for subsurface ice on Mars. *Planetary and Space Science* 85, 53-58.
613 Hemingway, J.D., Rothman, D.H., Grant, K.E., Rosengard, S.Z., Eglinton, T.I., Derry, L.A., and
614 Galy, V.V. (2019). Mineral Protection Regulates Long-Term Global Preservation of
615 Natural Organic Carbon. *Nature* 570, 228-231.
616 Hayes, J.M. (2001). Fractionation of the Isotopes of Carbon and Hydrogen in Biosynthetic
617 Processes. *Geochem. Cosmochim. Acta* 65.
618 Hays, L.E., *et al*. (2017). Biosignature Preservation and Detection in Mars Analog Environments.
619 *Astrobiology* 17(4), 363-400.

620 Hunter, J.D. (2007). Matplotlib: A 2D Graphics Environment. *Computing in Science and*
621 *Engineering* 9(3), 90-95.
622 Hynek, B.M., Rogers, K.L., Antunovich, M., Avard, G., and Alvarado, G.E. (2018). Lack of
623 Microbial Diversity in an Extreme Mars Analog Setting: Poas Volcano, Costa Rica.
624 *Astrobiology* 18(7), 923 - 933.
625 Jenkins, O.P. (1918). Spotted Lakes of Epsomite in Washington and British Columbia. *Am. J. Sci.*
626 46, 638-644.
627 Jepsen, S.M. Priscu, J.C., Grimm, R.E., and Bullock, M.A. (2007). The Potential for
628 Lithoautotrophic Life on Mars: Application to Shallow Interfacial Water Environments.
629 *Astrobiology* 7(2), 342-354.
630 Johnson, D.B., Beddows, P.A., Osburn, M.R. (2018). Microbial Diversity and Biomarker Analysis
631 of Modern Freshwater Microbialites from Laguana Bacalar, Mexico. *Geobiology* 16, 319-
632 337.
633 Johnson, S.S., *et al*. (2020). Lipid Biomarkers in Ephemeral Acid Salt Lake Mudflat/Sandflat
634 Sediments: Implications for Mars. *Astrobiology* 20(2), 167-178.
635 Kaneko, M., Kitajima, F., and Naraoka, H. (2011). Stable Hydrogen Isotope Measurement of
636 Archaeal Ether-Bound Hydrocarbons. *Organic Geochemistry* 42, 166-172.
637 Kite, E.S., Gaidos, E., & Onstott, T.C. (2018) Valuing Life Detection Missions. *Astrobiology*
638 18(7), 834-840.
639 Klempay, B., *et al*. (2021). Microbial Diversity and Activity in Southern California Salterns and
640 Bitterns: Analogues for Remnant Ocean Worlds. *Environmental Microbiology*, 23(7),
641 3825-3839.
642 McFarlin, J.M., Axford, Y., Masterson, A.L., Osburn, M.R. (2019). Calibration of Modern
643 Sedimentary δ^2H Plant Wax-Water Relationships in Greenland Lakes. *Quaternary Science*
644 *Reviews* 225.
645 Mesbah, N.M., and Wiegel, J. (2008). Life at Extreme Limits The Anaerobic Halophilic
646 Alkalithermophiles. *Ann N.Y. Acad. Sci.* 1125, 44-57.
647 Meyers, P.A., *et al*. (1980). Hydrocarbons and Fatty Acids in Two Cores of Lake Huron Sediments.
648 *Geochimica et Cosmochimica Acta* 43, 1215 - 1221.
649 Meyers, P.A. (1994). Preservation of Elemental and Isotopic Source Identification of Sedimentary
650 Organic Matter. *Chemical Geology* 114, 289 - 302.

Meyers, P.A. (2003). Applications of organic geochemistry to paleolimnological reconstructions: a summary of examples from the Laurentian Great Lakes. *Organic Geochemistry* 34, 261 - 289.

Middleburg, J.J., (1989). A Simple Rate Model for Organic Matter Decomposition in Marine Sediments. *Geochim. Cosmo. Acta* 53, 1577-1581.

Middleburg, J.J., *et al*. (1993). Organic Matter Mineralization in Marine Systems. *Global and Planetary Change* 8, 47-58.

Moreras-Marti, A., Fox-Powell, M., Zerkle, A.L., Stueeken, E., Gazquez, F., Brand, H.E., Galloway, T., Purkamo, L., and Cousins, C.R. (2021). Volcanic Controls on the Microbial Habitability of Mars-Analogue Hydrothermal Environments. *Geobiology* 19, 489 - 509.

Naghoni, A., *et al*. (2017). Microbial Diversity in the Hypersaline Lake Meyghan, Iran. *Scientific Reports* 7(11522).

O'Connor, B.R.W., Fernandez-Martinez, M.A., Leveille, R.J., and Whyte, L. (2021). Taxonomic Characterization and Microbial Activity Determination of Cold-Adapted Microbial Communities in Lava Tube Ice Caves from Lava Beds National Monument, a High-Fidelity Mars Analogue Environment. *Astrobiology* 21(5), 613 - 627.

Oksanen J. F., Blanchet G., Friendly M., Kindt R., Legendre D. M., Minchin P. R., O'Hara R. B., Simpson G. L., 779 Solymos P., Stevens M. H. H. and others. (2019) vegan: Community Ecology Package.

Perry, G.J., Volkman, J.K., & Johns, R.B. (1979). Fatty Acids of Bacterial Origin in Contemporary Marine Sediments. *Geochimica et Cosmochimica Acta* 43, 1715 - 1725.

Pontefract, A., Zhu, T., Walker, V.K., Hepburn, H., Lui, C., Zuber, M.T., Ruvkun, G., and Carr, C.E. (2017). Microbial Diversity in a Hypersaline Sulfate Lake: A Terrestrial Analog of Ancient Mars. *Front. Microbiol.* 8:1819.

Popa, R., Smith, A.R., Popa, R., Boone, J., and Fisk, M. (2012). Olivine-Respiring Bacteria Isolated from the Rock-Ice Interface in a Lava-Tube Cave, a Mars Analog Environment. *Astrobiology* 12(1), 9 - 18.

Renaut, R., and Long, P. (1989). Sedimentology of the Saline Lakes of the Cariboo Plateau, Interior British Columbia, Canada. *Sedimentary Geology* 4, 239-264.

Renaut, R. (1993). Morphology, Distribution, and Preservation Potential of Microbial Mats in the Hydromagnesite-Magnesite Playas of the Cariboo Plateau, British Columbia, Canada. *Hydrobiologia* 267, 75-98.

Rivera-Valentin, E.G., *et al*. (2020). Distribution and Habitability of (Meta)stable Brines on Present-Day Mars. *Nature Astronomy.*

Robinson, J.L., *et al*. (2005). Growth Kinetics of Extremely Halophilic *Archaea* (Family *Halobacteriaceae*) as Revealed by Arrhenius Plots. *J Bacteriol* 187(3), 923-929.

Sam, L., Bhardwaj, A., Singh, S., Martin-Torres, F.J., Zorzano, M.P., and Ramirez Luque, J.A. (2020). Small Lava Caves as Possible Exploratory Targets on Mars: Analogies Drawn from UAV Imaging of an Icelandic Lava Field. *Remote Sens.* 12(1970).

Schimmelmann, A., *et al.* (2009). Nicotine, Acetanilide and Urea Multi-Level ^{2}H-, ^{13}C- and ^{15}N-Abundance Reference Materials for Continuous-Flow Isotope Ratio Mass Spectrometry. *Rapid Communications in Mass Spectrometry*. 23, 3513-3512.

Schouten, S., Hopmans, E.C., and Sinnighe Damste, J.S. (2013). The Organic Geochemistry of Glycerol Dialkyl Glycerol Tetraether Lipids: A Review. *Organic Geochemistry* 54, 19-61.

Schouten, S., *et al*. (2010). Fossilization and Degradation of Intact Polar Lipids in Deep Subsurface Sediments: A Theoretical Approach. *Geochim. Cosmo. Acta* 74, 3806-3814.

Shen, J., Zerkle, A.L., and Claire, M.W. (2022). Nitrogen Cycling and Biosignatures in a Hyperarid Mars Analog Environment. *Astrobiology* 22(2), 127 - 142.

Sobron, P., Wang, A., Mayer, D.P., Bentz, J., Kong, F., Zheng, M. (2018). Dalangtan Saline Playa in a Hyperarid Region of Tibet Plateau: III. Correlated Multiscale Surface Mineralogy and Geochemistry Survey. *Astrobiology* 18(10), 1277 - 1304.

Sohlenkamp, C., and Geiger, O. (2016). Bacterial Membrane Lipids: Diversity in Structures and Pathways. *FEMS Microbiology Reviews* 40, 133-159.

Tan, J., Lewis, J.M.T., and Sephton, M.A. (2018). The Fate of Lipid Biosignatures in a Mars-Analogue Sulfur Stream. *Scientific Reports* 8:7586.

Tan, J., and Sephton, M.A. (2020). Organic Records of Early Life on Mars: The Role of Iron, Burial, and Kinetics on Preservation. *Astrobiology* 20(1).

Tosca, N.J., Knoll, A.H., McLennan, S.M. (2008). Water Activity and the Challenge for Life on Mars. *Science* 320(5880), 1204-1207.

Wickham, H (2016). ggplot2: Elegant Graphics for Data Analysis. Springer-Verlag New York. ISBN 978-3-319-24277-4

Wilhelm, M.B., Davia, A.F., Eigenbrode, J.L., Parenteau, M.N., Jahnke, L.L., Liu, X.L., Summons, R.E., Wray, J.J., Stamos, B.N., O"Reill, S.S., Williams, A. (2017). Xeropreservation of Functionalized Lipid Biomarkers in Hyperarid Soils in the Atacama Desert. *Organic Geochemistry*, 103, 97-104.

Willers, C., *et al*. (2015). Phospholipid Fatty Acid Profiling of Microbial Communities - A Review of Interpretations and Recent Applications.